

Bayesian Compressive Sensing Based Evolutionary Power Spectrum Estimation for Incomplete Process Records

S. Kruse¹, E. Patelli^{1,2} and M. Beer^{1,3,4}

¹*Institute for Risk and Uncertainty, University of Liverpool, Liverpool, UK. Email: s.kruse@liverpool.ac.uk*

²*Civil and Environmental Engineering, Strathclyde University, Glasgow, UK. Email: edoardo.patelli@strath.ac.uk*

³*Institute for Risk and Reliability, Leibniz Universität Hannover, Hanover, Germany. Email: beer@irz.uni-hannover.de*

⁴*International Joint Research Center for Engineering Reliability and Stochastic Mechanics (ERSM), Tongji University, Shanghai, China*

Abstract: A Bayesian compressive sensing (BCS) based approach for estimating evolutionary power spectral density functions of non-stationary stochastic processes based on problematic data records is developed. In particular, a detailed derivation of generalized harmonic wavelet bases for the compact representation of non-stationary environmental processes measured on finite intervals is presented. This representation leads, next, to an evolutionary power spectrum estimation approach. In the presence of missing data, BCS can be employed to determine the required wavelet coefficients and to quantify the induced reconstruction uncertainties. Finally, a computationally efficient method for applying BCS to the application-specific optimization problems is introduced. A numerical example suggests that the proposed approach offers accurate estimation and propagates the inherent uncertainties reliably.

Keywords: Discrete generalized harmonic wavelet transform, Bayesian compressive sensing, Evolutionary power spectra, Missing data.

1. Introduction

The ability to model the performance of engineering structures that operate in dynamic environments (i.e. offshore wind turbines) is a requirement to assure the reliability and the availability of such systems and informing design decisions. Computer-based dynamic models rely on the capability of accurate estimation of environmental excitations. Hence, a clear understanding of the variations in operational and ambient conditions expected for the structures is of main interest. However, estimating statistical properties of stochastic processes associated with physical loads is particularly challenging in the light of corrupted or partially missing data. Reasons for problematic data can be sensor failures, bandwidth limitations or operating range exceedance of sensors in extreme operational conditions (Comerford et al. 2017).

The time-varying frequency content of non-stationary stochastic processes can be characterized and modeled in terms of evolutionary power spectral density functions (Priestley 1967). In this regard, Evolutionary Power Spectra (EPS) generalize the physical meaning of traditional power spectra density functions which are appropriate only for stationary processes. Considering the problem of estimating EPS, a wavelet transform based approach has turned out to overcome certain limitations of other methods such as the Wigner-Ville method and window based schemes due to the beneficial properties of wavelets (Spanos and Failla 2004). Latter are the reason why wavelet analysis has found its way also into other fields of engineering. Further research efforts have focused on estimating EPS in the presence of missing data. Particularly worth highlighting is a Compressive Sensing (CS) based approach demonstrating superior performance compared with other state-of-the-art techniques (Comerford et al. 2016, Comerford et al. 2017). Here, the wavelet coefficients are determined following the signal

processing concept of CS given a problematic signal of interest. The underlying signals can then be reconstructed and the EPS estimated.

One point of criticism is the lack of information about the basis used to represent the signal. In particular, it is important to distinguish between the continuous and the discrete wavelet transform. Inasmuch as the discrete wavelet coefficients cannot offhand be utilized in the estimation formula derived for the continuous case. For this reason, the first part of the present paper provides a detailed derivation of the orthogonal wavelet basis with clearer notation.

Another limitation of the CS based approach is the need to quantify uncertainties of the load characterization caused by the loss of information. This can be achieved by utilizing the framework of Bayesian Compressive Sensing (BCS), see e.g. (Ji et al. 2008). Attacking the sparse regression tasks from a Bayesian perspective provides posterior distributions for each of the basis coefficients naturally quantifying reconstruction uncertainties, instead of modest point estimates. Beyond that, enhanced variants have been proposed, e.g. (Huang et al. 2016), showing more robust performance in case of only approximately sparse signals and exploit statistical relationships between different data sets (Ji et al. 2009).

This paper presents a novel approach for estimating the evolutionary power spectral densities of non-stationary stochastic processes based on problematic data records. In this context the remaining sections are structured as follows. As described above, section 2 initially derives the orthogonal wavelet basis for discrete signals measured on a finite range and elucidates the relationship between resulting coefficients and the EPS. Section 3 includes a brief review of CS and introduces a computational efficient way to apply BCS to the complex-valued optimization problem. The paper concludes with a numerical example,

which suggests that the proposed approach offers sufficiently accurate estimation and propagates the inherent uncertainties reliably.

2. Wavelet Analysis

This section concisely includes the theory of wavelet-based EPS estimation. By representing arbitrary functions utilizing families of wavelets, one is able to decompose these functions into time-frequency space. In this way variations of power can be analyzed locally in time.

2.1 Generalized Harmonic Wavelets

An exceptional family of wavelets are the generalized harmonic wavelets (GHW). Each of these complex-valued functions $w_{(m,n),(k)}(t)$ is defined by three parameters. The first two determine the scale and prescribe the frequency range of the GHW. The third parameter specifies its position in time. More precisely, k shifts the function. GHW feature a box-shaped frequency spectrum. Originally developed to precisely achieve this manipulable band-limited property (Newland 1993), this structure simplifies the exploration of frequency specific content. If the parameters are chosen appropriately, the family of GHW provides a complete set of orthogonal basis functions for signal analysis (Newland 1994a).

2.2 Circular Generalized Harmonic Wavelets

Unfortunately, aforementioned theory holds only true for (continuous) functions defined on an infinite domain. The reason is that GHW do not form a set of orthogonal basis functions on a finite interval (Spanos et al. 2016). Since no measured signal can fulfill this condition, the present paper employs periodization of GHW to make ensuing analysis implementable. Circular or periodized GHW (PGHW) with period T_0 are defined (Daubechies 1992, Newland 1993, 1994a, Spanos et al. 2016) as infinite sum of this wavelet shifted by multiples of T_0 . In this manner, the finite energy of the wavelet, which exists beyond the considered time period $[0, T_0]$, is transmitted into this interval. Transformations provide the analytical representation

$$w_{(m,n),(k)}^c(t) := \frac{1}{n-m} \sum_{q=m}^{n-1} e^{i\Delta_\omega q(t - \frac{kT_0}{n-m})}, \quad (1)$$

with $\Delta_\omega := 2\pi/T_0$. Note, that the summation index derived here dissent from the representation in (Spanos et al. 2016). As can readily be seen, PGHW are sums of harmonic functions with underlying frequencies of $m\Delta_\omega, \dots, (n-1)\Delta_\omega$. Compatible with this observation, the Fourier transformation of Eqn. 1 reveals the PGHW in the frequency domain

$$W_{(m,n),(k)}^c(\omega) := \frac{1}{n-m} \sum_{q=m}^{n-1} e^{-i2\pi q \frac{kq}{n-m}} \cdot \delta(\omega - q\Delta_\omega). \quad (2)$$

2.3 Discrete Generalized Harmonic Wavelet Transform

Since measurements in real-life applications as a rule provide time-discrete signals, this paper exclusively considers sampled functions $f_r := f(t = r \cdot \Delta_t)$, $r = 0, \dots, N_0 - 1$ hereinafter, with $\Delta_t := T_0/N_0$. For this case,

the discrete harmonic wavelet transformation (DGHWT) is deduced as

$$a_{(m,n),(k)}^{dc} := \frac{1}{N_0} \sum_{r=0}^{N_0-1} f_r \sum_{q=m}^{n-1} e^{i2\pi q(\frac{k}{n-m} - \frac{r}{N_0})}. \quad (3)$$

Note that Eqn. 3 generalizes the discrete Fourier transformation (DFT), e.g. (Newland 1994b). Both definitions correspond for $s = m$ and band width 1. The wavelet representation of the discrete function using PGHW results as

$$f_r = \sum_{l=1}^L \sum_{k=0}^{b_l} a_{(m_l, n_l),(k)}^{dc} \cdot w_{(m_l, n_l),(k)}^c(r \cdot \Delta_t), \quad (4)$$

where $1 \leq L \leq N_0$ depicts the number of frequency bands with $b_l := n_l - m_l - 1$. Furthermore, Eqn. 4 gives the inverse DGHWT respectively. The partition of the wavelet coefficients $P := [m_1, n_1; m_2, n_2, \dots, m_L, n_L]$, with $m_1 = 0$, $n_L = N_0$ and $n_l = m_l - 1$ for $l = 2, \dots, L$ controls the trade-off between time and frequency resolution of the ensuing analysis. Depending on the objective of the application, P can be chosen as required. Beyond that, the Fourier coefficients of the input sequence can be expressed by means of the DFT of the wavelet coefficients in turn

$$F_s = \frac{1}{n_l - m_l} \sum_{k=0}^{b_l} a_{(m_l, n_l),(k)}^{dc} \cdot w_{(m_l, n_l),(k)}^c(r \cdot \Delta_t), \quad (5)$$

with $s = m_l, \dots, n_l - 1$. These operations can be combined for all frequency bands in a single block diagonal matrix W_P . Therefore, the inverse problem

$$f = \mathfrak{F}^{-1} \cdot W_P \cdot a =: \Psi_P \cdot a \quad (6)$$

reveals the structure of the searched for orthogonal PGHW basis Ψ_P . In the aforementioned equation, \mathfrak{F}^{-1} depicts the inverse DFT matrix and the vector a consists of all PGHW coefficients. The orthogonality of the DFT matrices in conjunction with the block diagonal shape of W_P yields the orthogonality of the derived basis matrix.

It is worth noting, that the vector a constitutes an approximation (Newland 1994c) of the GHW coefficients of the truncated wavelet representation (Newland 1994a). In this context, the Nyquist frequency enforces the truncation.

3. Evolutionary Power Spectra Estimation

Concerning the problem of estimating EPS $S(\omega, t)$ of non-stationary stochastic processes, (Spanos and Kougioumtzoglou 2012) and (Wang 2018) derived in different ways the GHW based formula

$$\bar{S}(\omega_l, t_k) = \frac{E[|a_{(m,n),(k)}|]^2}{\Delta_\omega(n-m)}, \quad (7)$$

with $m\Delta_\omega \leq \omega_l < n\Delta_\omega$ and $\frac{k}{n-m}T_0 \leq t_k < \frac{k+1}{n-m}T_0$. More precisely, Eqn. 7 is the averaged EPS over the frequency-time interval $[m\Delta_\omega, n\Delta_\omega] \times [\frac{k}{n-m}T_0, \frac{k+1}{n-m}T_0)$ (Wang 2018). Considering wavelet maps (e.g. Newland 1994a), the PGHW based formula can be derived

analogously to (Spanos and Kougioumtzoglou 2012). Regarding discrete finite and non-stationary stochastic processes, EPS estimation results as

$$\bar{S}(\omega_l, t_k) = \frac{4E[|a_{(m,n)(k)}^{dc}|]^2}{(n-m)}, \quad (8)$$

with $m\Delta_\omega \leq \omega_l < n\Delta_\omega$ and $\frac{k}{n-m}T_0 \leq t_k < \frac{k+1}{n-m}T_0$. Note that Eqn. 8 matches the estimate in (Spanos et al. 2005). In practice, the expected value is estimated by means of available realizations (measurements) of the stochastic process under consideration.

4. Compressive Sensing

Compressive sensing (CS) is a branch of signal processing which has become a research field under great attention. On condition that a signal is sufficient sparse in any incoherent transform domain, CS enables reconstruction of this signal notwithstanding a significantly reduced number of required incoherent measurements, even below the Nyquist rate. In this context, (approximative) signal sparsity means, that only a few dominant coefficients can represent the underlying signal in an orthogonal transform basis. CS covers not only compressed sensing, i.e. strategies to acquire a significantly reduced number of data directly compressed at the sensor, but also the theory of their traceability as well as algorithms to reconstruct the signal (e.g. Donoho 2006).

Missing data can be understood as unintentionally additional compression. This involuntarily character unfortunately withdraws the control from the sensing process. Depending on its distribution, the probability of a successful reconstruction deteriorates. In this regard, large connected sequences of missing data impose escalating uncertainty and worsen the results. Nevertheless, CS already demonstrates comparatively strong performance in the considered cases of missing data (Comerford et al. 2016, Comerford et al. 2017).

Next, consider the situation of a given compressed sensing strategy including data loss. In this context, the so-called measurement matrix Φ projects a regularly sampled underlying signal f onto the actually measured one g . The first matrix in Fig. 1 reveals the structure of Φ in the case of 50% uniformly distributed missing data points without further compression. Since the underlying signal is presumed to be sparse, the vector ω can represent f relative to Ψ . All in all, this results in the under-determined system of linear equations with the compressive sensing matrix Θ .

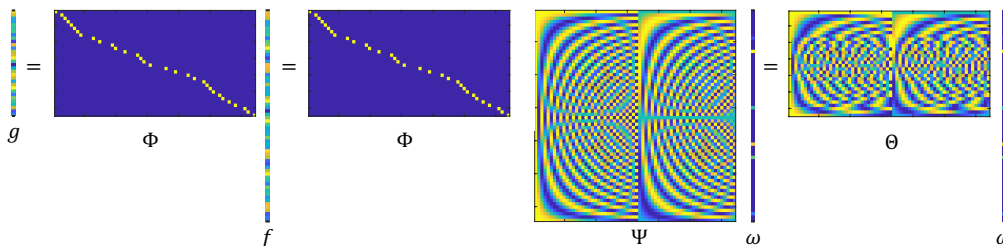


Figure 1: Compressive sensing framework in the context of missing data. This basis is the split DFT matrix according to the procedure described in subsection 4.3.

The basic idea of CS, utilizing the properties sparsity and incoherency, to reconstruct ω (and thus f) by solving the optimization problem

$$\min_{\omega} \|\omega\|_0 \quad s. t. \quad \|g - \Theta\omega\|_2 \leq \epsilon \quad (9)$$

with ϵ small in the presence of noise. Unfortunately, Eqn. 9 is a NP-hard problem. For this reason, algorithms simply seek a good match for the sparsest solution, mostly by relaxing the norm and solving the resulting convex optimization problem in a simple way (Orović et al. 2016).

4.1 Bayesian Compressive Sensing

Bayesian Compressive Sensing is a certain class of solution algorithm. Here, the constraint of the CS optimization problem is understood as Bayesian linear regression task. With the aid of a sparse-promoting prior, the solution of the optimization problem is provided as a posterior distribution for the coefficients. Quantification of the reconstruction uncertainty is determined by means of error bars, which correspond to the standard deviation around the expected value. This framework is also known as sparse Bayesian learning and Relevance Vector Machine. Further, (Ji et al. 2008) proposes a hierarchical Bayesian framework which provides a conjugate prior. The posterior results as multidimensional normal distribution, which can be calculated analytically given the hyperparameters. Furthermore, the propagated distribution of the reconstructed signal can be determined by means of simple matrix multiplications. For the sake of efficiency, an empirical Bayesian procedure is employed to point estimate the hyperparameters in a fast manner. If this is based on several data sets, we speak of multi-task BCS (MTBCS) (Ji et al. 2009). MTBCS tries to exploit presumed correlation between the sets. The single-task variant is hereinafter referred to as STBCS.

MATLAB code of an accelerated version is available online at <https://github.com/shihaoji/bcs> and used to run BCS in the next chapter. See (Ji et al. 2009).

4.2 Application-specific BCS

Both the DGHWT matrix derived in section 2.3 and the wavelet coefficients are complex-valued consequently. For this reason, the posterior distribution to be determined must be complex normally distributed.

A natural choice is to reformulate the CS problem as $2N_0$ -dimensional real-valued one. The subsequent application of BCS yields the desired distribution for $X = [U^T, V^T]^T$, where U represents the real and V the imaginary part of the coefficient vector. This procedure is referred to as CBCS hereinafter.

To prevent such an inflation of the dimension, this section introduces a more computationally efficient variant. First, the real and imaginary parts of the CS matrix Θ form a new matrix R . This matrix is then used to determine the row reduced echelon form E

$$R := [Re(\Theta) \quad Im(\Theta)] \rightarrow E := [E_1 \quad E_2]. \quad (10)$$

With the help of E it is easy to identify N_0 columns of R which span a real-valued basis Y . The remaining N_0 columns of R can be expressed as linear combinations of the columns of Y . Applying BCS to the proxy problem with new CS matrix Y yields a N_0 -dimensional normal distribution with expected value μ_Y and covariance matrix Σ_Y .

Assuming X is $2N_0$ -dimensional normally distributed as in CBCS, its expected values μ_U , μ_V and the covariance matrix Σ_X result as

$$\mu_X = \begin{bmatrix} \mu_U \\ \mu_V \end{bmatrix} = \begin{bmatrix} E_1 & -E_2 \\ E_2 & E_1 \end{bmatrix}^{-1} \begin{bmatrix} \mu_Y \\ 0 \end{bmatrix}, \quad (11)$$

$$\Sigma_X = \begin{bmatrix} E_1 & -E_2 \\ E_2 & E_1 \end{bmatrix}^{-1} \begin{bmatrix} \Sigma_Y & 0 \\ 0 & 0 \end{bmatrix} \begin{bmatrix} E_1 & -E_2 \\ E_2 & E_1 \end{bmatrix}^{-1T}. \quad (12)$$

Note that the respective solutions generally do not correspond. This is not an issue in so far as both are sparse and physically meaningful solutions to the optimization problem.

In addition, the invertibility of the matrix remains to be shown in general.

Once the posterior distribution of X is determined, the resultant distribution of EPS can be propagated through Eqn. 8 by means of Monte Carlo simulation. While doing so, merely normally distributed samples need to be drawn.

5. Numerical Example

In this section the BCS based EPS estimation approach is applied to simulated earthquake time histories. Their underlying non-stationary stochastic process is characterized by the non-separable EPS (Spanos and Kougioumtzoglou 2012; see also Comerford et al. 2016)

$$S(\omega, t) = \left(\frac{\omega}{5\pi}\right)^2 e^{(-0.15t)t^2} e^{-\left(\frac{\omega}{5\pi}\right)^2 t}. \quad (13)$$

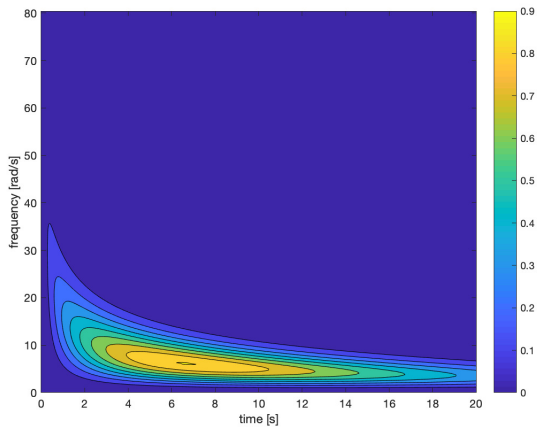


Figure 2: Non-separable underlying spectrum plotted from Eqn. 13.

Fig. 2, shows the spectrum directly plotted from Eqn. 13. During the first seconds Eqn. 13 has a relatively broad spectrum of power. However, the width of the frequency band decreases rapidly and stabilizes evolutionary over the remaining period under consideration. The greatest concentration of energy/power is evident between second 6 and 7 in a relatively low frequency range.

First, process records compatible with the underlying EPS are generated utilizing the concept of spectral representation (Liang et al. 2007). Concerning this matter, a non-stationary stochastic process with zero mean can be represented by an infinite sum of EPS evaluations and independent uniformly distributed random phase angles. Truncation of this sum together with realizations of the involved random variables yields an even sampled simulation of the stochastic process with great computational efficiency. By this means, a total number of 500 process records are simulated with $N_0 = 512$ sample points each at a period of $T_0 = 20$. This choice results in a Nyquist frequency of $\omega_N = 80.42$ [rad/s].

In the following examples, estimations are based on PGHW coefficients according to Eqn. 8. To obtain a well-balanced time-frequency resolution, a wavelet basis Eqn. 6 with equidistant partition of $n - m = 16$ is chosen. Altogether this corresponds to a resolution of $\Delta_{(m,n)} = 5.03$ [rad/s] in the frequency and $\Delta_{(k)} = 1.25$ [s] in the time domain.

Fig.4 depicts the PGHW based EPS estimation without missing data based on the simulated process records.

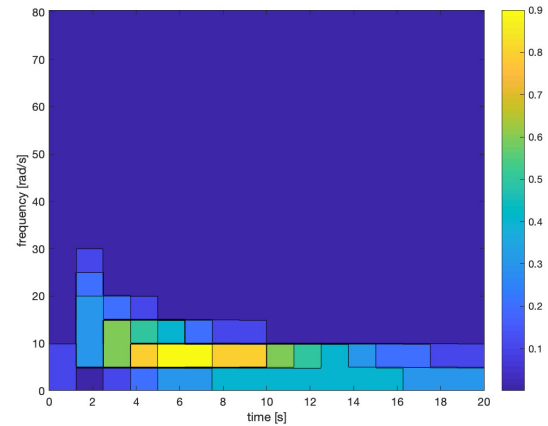


Figure 3: EPS estimation acc. to Eqn. 8 based on 500 process records without missing data.

In light of the inevitable partitioning, Eqn. 8 provides an accurate estimation of Eqn. 13. Although the power peak is overestimated in terms of surface area, location and magnitude of the identified frequencies are correct. Likewise, Fig. 3 captures the evolutionary structure of the underlying EPS clearly. The erroneously detected low frequencies at the beginning can be explained by the leakage effect. Note that a more appropriate partition, which requires in a sense knowledge of the underlying EPS, would improve the result. To that effect, high frequency definition in the lowest frequencies reduces the

plot to zero. This is possible as no time resolution is needed there. In the same way, a higher resolution in time at the beginning of the process is able to capture the fast evolution in the higher frequencies better.

Note that each of the squares in Fig. 3 corresponds to an identified wavelet coefficient. It is common to render interpolated plots. The resulting images show more realistic EPS estimations. However, they do not conform to Eqn. 8. Post-processing of the estimations is beyond the scope of this paper. Due to the limitations described above, Fig. 3 is considered the target spectrum for the case of missing data.

Next, the loss of data is simulated. Per record 160 out of 512 data points are deleted independently of each other in uniformly distributed locations. This equals 31.25% missing data.

STBCS and MTBCS are employed to estimate the underlying EPS based on the ensemble of process records with imposed missing data. Fig. 4 and 5 show the absolute differences to the target spectrum Fig. 2.

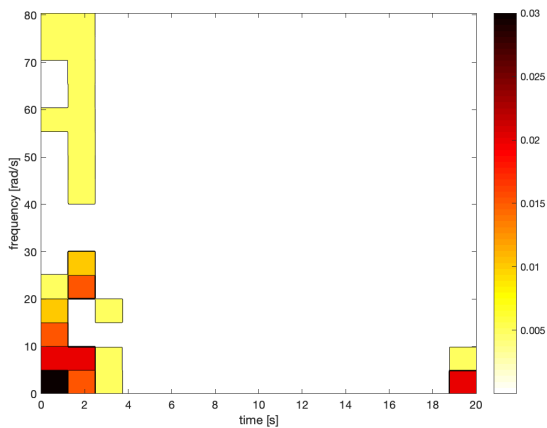


Figure 4: Error of the STBCS based EPS estimation with 500 process records and 31.25% missing data.

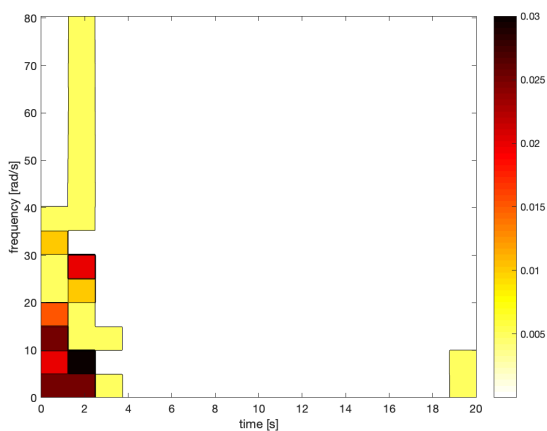


Figure 5: Error of the MTBCS based EPS estimation with 500 process records and 31.25% missing data.

Despite the lack of information due to the missing data, both methods demonstrate excellent results. In this

example the accumulated error is slightly smaller for STBCS. Furthermore, Fig. 6 and 7 show these outcomes combined with their propagated error bounds.

As can easily be seen, STBCS quantifies and propagates the uncertainty induced by missing data more realistically than MTBCS. Not only does the STBCS have significantly lower error bounds, but its quantile completely encloses the target spectrum, in contrast to MTBCS. Other constellations of missing data (e.g. in small intervals) with the same realizations strengthen these observations. A potential explanation for larger error bounds and their chaotic arrangement in MTBCS is a pronounced variability of EPS estimates within individual realizations. However, this remains to be investigated.

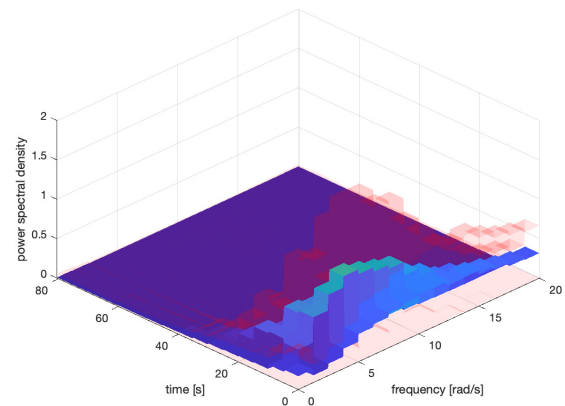


Figure 6: Error bars (quasi-transparent red) of the STBCS based EPS (blue) estimation (blue) with 500 process records and 31.25% missing data.

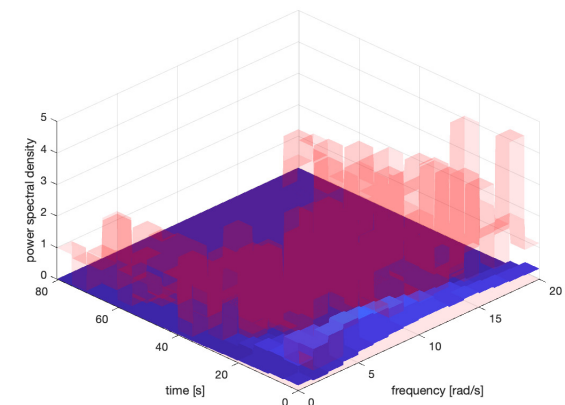


Figure 7: Error bars (quasi-transparent red) of the MTBCS based EPS estimation (blue) with 500 process records and 31.25% missing data.

6 Conclusions

In this paper, a BCS and DGHWT based approach for evolutionary power spectrum estimation in the presence of missing data has been proposed. In particular, the orthogonal DGHWT matrix has been deduced, which directly enables a further processing and its

interpretability. Relying on the properties of circular GHW, a relationship between their coefficients and EPS has been derived. The example demonstrates the quality/capacity of this estimation method in the case of non-stationary stochastic processes discretely realized on a finite interval. Further, the proposed proxy optimization problem and the subsequent ascription allow for an efficient application of BCS for EPS estimation. The numerical example suggests, that STBCS is an appropriate method for both EPS estimation and quantifying the reconstruction uncertainties in the presence of missing data. The multitask approach, on the other hand, performs inferiorly, at least in the application case. Reasons for this remain to be investigated.

In this regard, further work is planned on modifying the hierarchical framework of the BCS. On the one hand, the advantages of the multitask approach shall be exploited (in the context of EPS) and on the other hand, side information shall be incorporated into the reconstruction process. Latter is intended to counteract escalating uncertainties, which may occur due to large sequences of missing data.

Acknowledgement



This project has received funding from the European Union's Horizon 2020 research and innovation programme under the Marie Skłodowska-Curie grant agreement No 764547.

References

- Comerford, L.A., Jensen, H.A., Mayorga, F. Beer, M. and Kougoumtzoglou, I.A. 2017. Compressive sensing with an adaptive wavelet basis for structural system response and reliability analysis under missing data. *Computers and Structures*, 182: 26-40.
- Comerford, L.A., Kougoumtzoglou, I.A. and Beer, M. 2016. Compressive sensing based stochastic process power spectrum estimation subject to missing data. *Probabilistic Engineering Mechanics*, 44: 66-76.
- Daubechies, I. 1992. Ten Lectures on Wavelets. *Society for Industrial and Applied Mathematics*.
- Donoho, D.L. 2006. Compressed sensing. *IEEE Transactions on Information Theory*, 52(4): 1289-1306.
- Huang, Y., Beck, J. L., Wu, S. and Li, H. 2016. Bayesian compressive sensing for approximately sparse signals and application to structural health monitoring signals for data loss recovery. *Probabilistic Engineering Mechanics*, 46: 62–79.
- Ji, S., Dunson, D. and Carin, L. 2009. Multitask compressive sensing. *IEEE Transactions on Signal Processing*, 57(1): 92-106.
- Ji, S., Xue, Y. and Carin, L. 2008. Bayesian compressive sensing. *IEEE Transactions on Signal Processing*, 56(6): 2346-2356.
- Liang, J., Chaudhuri, S.R. and Shinozuka, M. 2007. Simulation of nonstationary stochastic processes by spectral representation. *Journal of Engineering Mechanics*, 133(6): 616-627.
- Newland, D.E. 1993. Harmonic wavelet analysis. In *Proceedings of the Royal Society of London, Series A: Mathematical and Physical Sciences*, 443(1917): 203-225.
- Newland, D.E. 1994a. Harmonic and musical wavelets. In *Proceedings of the Royal Society A: Mathematical, Physical and Engineering Sciences*, 444(1922): 605-620.
- Newland, D.E. 1994b. An Introduction to Random Vibrations, Spectral and Wavelet Analysis. *Longman Group UK Ltd*.
- Newland, D.E. 1994c. Wavelet analysis of vibration: Part 1 - Theory. *Journal of Vibration and Acoustics*, 116(4): 409-416.
- Orović, I., Papić, V., Ioana, C., Li, X. and Stanković, S. 2016. Compressive sensing in signal processing: Algorithms and transform domain formulations. *Mathematical Problems in Engineering*, 2016: 1-16.
- Priestley, M.B. 1967. Power spectral analysis of non-stationary random processes. *Journal of Sound and Vibration*. 6(1): 86–97.
- Spanos, P. D. and Failla, G. 2004. Evolutionary Spectra Estimation Using Wavelets. *Journal of Engineering Mechanics*. 130(8):952–960.
- Spanos, P.D., Tezcan, J. and Tratskas, P. 2005. Stochastic processes evolutionary spectrum estimation via harmonic wavelets. *Computer Methods in Applied Mechanics and Engineering*, 194(12-16): 1367-1383.
- Spanos, P.D. and Kougoumtzoglou, I.A. 2012. Harmonic wavelets based statistical linearization for response evolutionary power spectrum determination. *Probabilistic Engineering Mechanics*, 27(1): 57-68.
- Spanos, P.D., Kong, F., Li, J. and Kougoumtzoglou, I.A. 2016. Harmonic wavelets based excitation-response relationships for linear systems: A critical perspective. *Probabilistic Engineering Mechanics*, 44: 163-173.
- Wang, D., Fan, Z., Hao, S. and Zhao, D. 2018. An evolutionary power spectrum model of fully nonstationary seismic ground motion. *Soil Dynamics and Earthquake Engineering*, 105: 1-10.